Three-dimension deblurring algorithm for multiple observed images of moving object

Hong Hanyu, Fan Yan, Deng Zheyu, Shi Yu

(School of Electrical and Information Engineering, Wuhan Institute of Technology, Wuhan 430205, China)

Abstract: For the problem of deblurring of multiple observed images of moving objects with different blur kernels, a joint three-dimension deblurring method for multiple observed images was proposed. Unlike existing deblurring methods to remove 2D blur for single observed image without considering relationship of blur kernels in multiple observed images, the relationship of different PSF paths of multiple observed images was explored. The movement in three-dimension space was projected into each observed image planes, hence, the inherent relationship between the two PSF paths of two observed images can be set up. At first, motion blur kernels of two view images were estimated using single observed image debluring method and the blur kernels with one pixel width was refined. When having estimated two PSF paths, the other PSF paths could be calculated and optimized by using the relationship of PSF paths in multiple observed images. Then 3D blur of the observed images could be removed by using the proposed method. The experiment results for multiple observed images demonstrate that the proposed approach is efficient and effective in removing 3D blur and reconstruction.

Key words: object;　multiple observed images;　3D deblurring;　blur kernels relationship;
　　　　　　　3D reconstruction

动目标多视角观测图像的三维去模糊方法

洪汉玉,范　艳,邓哲煜,时　愈

(武汉工程大学 电气信息学院,湖北 武汉 430205)

摘　要: 当目标在多视角观测成像系统中有相对运动时, 所获取的多观测点图像是模糊的且各视角图像的模糊是不一样的,模糊核长度和方向都不同。针对这一问题,提出了多视角观测图像的三维去模糊方法。现有的图像去模糊方法主要是对单视角观测图像进行二维去模糊的,没有考虑目标多视角观测图像的模糊核之间的对应关系。文中从三维空间到二维观测面的映射关系出发,建立多视角观测图像的模糊路径之间的对应关系。先采用单观测图像去模糊的方法获取两视角观测图像的模糊核,并对模糊核进行精确化处理,得到单像素点宽的模糊核路径。再通过多视角观测图像模糊核路径之间的对应关系,估计其它观测图像的模糊核路径。最后,对多视角观测图像进行统一去模糊,并对去模糊

后的多视角观测图像进行三维重建。实验结果表明，文中方法能较好地去除目标多视角观测图像的三维模糊，提高了目标的三维重建质量。

关键词：目标；　多观测图像；　三维去模糊；　模糊核关系；　三维重建

0　Introduction

Recently, there has been a growing interest and some great developments in the stereo system and their 3D reconstruction. When objects have motions in spatial in the duration of short-exposure, the captured images are always blurred more or less caused by the movement of object. Even if we capture the images using the high-speed camera, the motion blur is not avoidable, and this makes the existing 3D reconstruction algorithms fail to reconstruct 3D object well.

The existing image deblurring methods can be classified into two main groups, single image deblurring methods[1-5] and multi-frame image deblurring methods[6-8]. Single image deblurring methods are not suit for multiple observed images deblurring, because they only remove 2D blur for single observed image. Multi-frame image deblurring methods using two or more images to perform blur estimation yield good estimation and deblurring results, but they need the same original image, thus limiting their application range. Recently, motional deblurring methods by using hybrid imaging system are proposed[9-10]. Hybrid camera system can captures two or three observed images by multiple cameras. However, it only needed to deblur the images of one view with high-resolution, with the aid of one or two cameras to estimate the blur kernel. From these works, we can know that existing methods do not concern the deblurring of multiple observations.

The major contribution of this paper is the foundation of relationship of multiple observation motional Point Spread Function (PSF) paths. When having estimated PSF paths of two observations, the PSF paths of the other observations can be calculated by using the relationship equations and refined by the

optimization. Then, the deblurring of the other observed images can be performed using our proposed method. Once getting all observations deblurring images with high quality, the 3D object can be easily reconstructed well by the existing 3D reconstruction methods.

1　Motional blur analysis in multiple observation system

A common multiple observation system is shown in Fig.1. When the object has a movement from P to Q in spatial coordinate system, its corresponding projection p_iq_i in every view imaging plane is shown in Fig.1. There are at least two main problems in multiple observation deblurring, one is that different observation has different direction motional blur, and another is that blur directions and lengths are different in each observation, that is to say blur kernel is different in each observation.
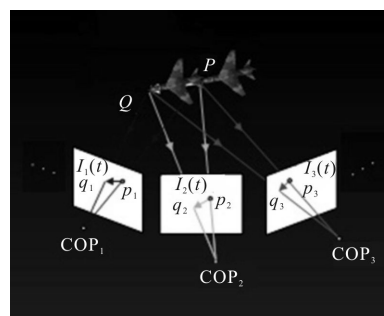

Fig.1 Moving object in multiple observation system

The observed image $g_i(x,y)$ can be expressed as following:

$$g_i(x,y)=h_i(x,y)\otimes f_i(x,y)+n_i(x,y),\ i=1,2,\cdots,N \quad (1)$$

where $g_i(x,y)$ represents the observed image, $h_i(x,y)$ is blur kernel (PSF) of observed image, $f_i(x,y)$ is projective latent image in observation plane, $n_i(x,y)$ is noise, $\otimes$ denotes discrete image convolution, and the subscript i denotes the observation number.

2 Refinement of PSF path

The oretically, the motional blur kernel is approximately a piece of line or a thin smooth curve, it can be used as knowledge guide for the blur kernel estimation.

In order to obtain PSF paths of two observed images for the following relationship exploited, we utilize blur kernel estimation algorithm based on preserving PSF path regularization[5], in which the nonquadratic regularization terms for both motional blur kernel and original image are incorporated in the iterative process.

After blur kernel estimated, we refine the blur kernel. The example of refinement of PSF path is shown in Fig.2.
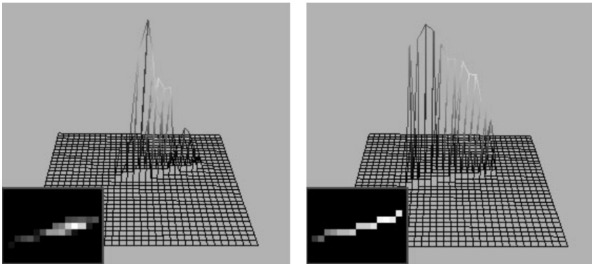
(a) Before refinement of PSF path (b) Refinement of PSF path

Fig.2 Refinement of PSF path

The main steps of the blur kernel refinement are listed following:

Step 1: Search the point with maximum value of PSF support as the current kernel point.

Step 2: Search the next kernel point in the $8-$ neighbor of the current kernel point to find their maximum and compare the direction consistency with previous kernel points. If there are two or more equal maximums, they are all regarded as candidates. The values of kernel points and the candidate remain in this iteration, the others are suppressed.

Step 3: When the value of the current point is too small or its direction is not consistent with the previous kernel points, stop searching; else go to Step 2.

3 Set up the relationship of PSF path in multiple observation planes

For simplicity, we first consider the linear motion

shown in Fig.3. Let P denote a 3×4 projection matrix. Let $(x\ y\ z\ 1)$ denote a homogeneous 3D coordinate of a point, and $(u\ v\ 1)$ denote a homogeneous 2D coordinate of its image projection, then $(x\ y\ z\ 1)$ and $(u\ v\ 1)$ are related by the following equation:

$$d\begin{pmatrix}u\\v\\1\end{pmatrix}=\begin{pmatrix}p_{00}&p_{01}&p_{02}&p_{03}\\p_{10}&p_{11}&p_{12}&p_{13}\\p_{20}&p_{21}&p_{22}&p_{23}\end{pmatrix}\begin{pmatrix}x\\y\\z\\1\end{pmatrix} \tag{2}$$

where d is the depth of the point with respect to the camera. P is camera parameter matrix, and the camera parametric projection matrix is defined by $K* [R\ t]$. Camera parameters K, $[R\ t]$ have been calculated in the process of multiple observation camera calibration.
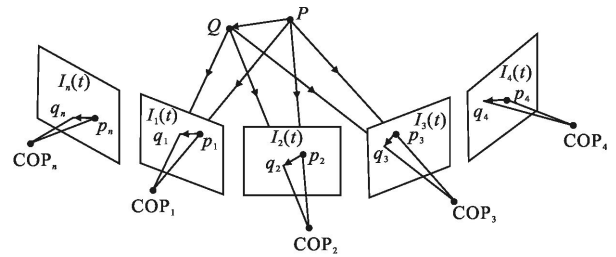

Fig.3 Multiple observation system

From Eq.(2) and Fig.3, it can be seen that the projection movement paths in each observation are different. We take two observations to set up the relationship of PSF paths. For convenience, we suppose the motion is uniform and the values of PSF are equal. Actually, the movement in spatial at the short exposure is very short and the distance between camera and object is far to compare object size, obviously, it is reasonable to suppose that motional PSF values and blur kernel direction are invariant for an image.

From Eq.(2), it is also known that if giving the values of a point $(x\ y\ z)$, we can get an unique set values of $(u\ v\ d)$, and vice versa. By performing matrix block-multiplication for Eq.(2) and shifting the vector $(x\ y\ z)^{\mathrm{T}}$ on the right-hand side of the equation to the left-hand side, we can obtain

$$\begin{pmatrix}x\\y\\z\end{pmatrix}=d[B]\begin{pmatrix}u\\v\\1\end{pmatrix}-[B]\begin{pmatrix}p_{03}\\p_{13}\\p_{23}\end{pmatrix} \tag{3}$$

where $[B]$ is the inverse matrix of $[P]_{3\times3}$, we have

$$[B]=\begin{vmatrix} p_{00} & p_{01} & p_{02} \\ p_{10} & p_{11} & p_{12} \\ p_{20} & p_{21} & p_{22} \end{vmatrix}^{-1} \qquad (4)$$

Below, we derive the projective movement displacment relation of two observations. When object moves from P to Q in 3D space, the projective point moves from $(u_0^{(i)}, v_0^{(i)})$ to $(u_1^{(i)}, v_1^{(i)})$ in 2D observation i, and from $(u_0^{(j)}, v_0^{(j)})$ to $(u_1^{(j)}, v_1^{(j)})$ in 2D observation simultaneously. Substituting $(u_1^{(i)}, v_1^{(i)})$ and $(u_0^{(i)}, v_0^{(i)})$, $(u_0^{(j)}, v_0^{(j)})$ and $(u_1^{(j)}, v_1^{(j)})$ to Eq.(5), respectively, we have

$$\begin{vmatrix} \Delta x \\ \Delta y \\ \Delta z \end{vmatrix} = d_1^{(k)}[B^{(k)}]\begin{vmatrix} u_1^{(k)} \\ v_1^{(k)} \\ 1 \end{vmatrix} - d_0^{(k)}[B^{(k)}]\begin{vmatrix} u_0^{(k)} \\ v_0^{(k)} \\ 1 \end{vmatrix} \qquad (5)$$

Letting $u_1^{(i)}=u_0^{(i)}+\Delta u^{(i)}$, $v_1^{(i)}=v_0^{(i)}+\Delta v^{(i)}$, and $u_1^{(j)}=u_0^{(j)}+\Delta u^{(j)}$, $v_1^{(j)}=v_0^{(j)}+\Delta v^{(j)}$, and using Eq.(5), we can set up the relationship equation between two observation i and observation j with respect to $(\Delta u^{(i)}, \Delta v^{(i)})$ and $(\Delta u^{(j)}, \Delta v^{(j)})$ as following:

$$d_1^{(i)}[B^{(i)}]\begin{vmatrix} u_0^{(i)}+\Delta u^{(i)} \\ v_0^{(i)}+\Delta v^{(i)} \\ 1 \end{vmatrix} - d_1^{(j)}[B^{(j)}]\begin{vmatrix} u_0^{(j)}+\Delta u^{(j)} \\ v_0^{(j)}+\Delta v^{(j)} \\ 1 \end{vmatrix} =$$

$$d_0^{(i)}[B^{(i)}]\begin{vmatrix} u_0^{(i)} \\ v_0^{(i)} \\ 1 \end{vmatrix} - d_0^{(j)}[B^{(j)}]\begin{vmatrix} u_0^{(j)} \\ v_0^{(j)} \\ 1 \end{vmatrix} = \begin{vmatrix} b_0 \\ b_1 \\ b_2 \end{vmatrix} \qquad (6)$$

Basically, the values of each observation PSF are just related with the vector of movement in observation, they are $psf_i=h(\Delta u^{(i)}, \Delta v^{(i)})$, $psf_j=h(\Delta u^{(j)}, \Delta v^{(j)})$, as shown in Fig.4.
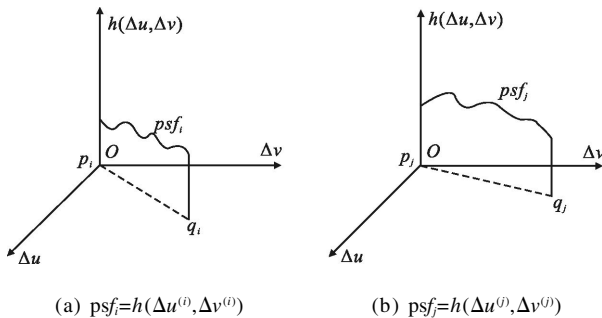
(a) $psf_i=h(\Delta u^{(i)}, \Delta v^{(i)})$ (b) $psf_j=h(\Delta u^{(j)}, \Delta v^{(j)})$

Fig.4 PSF paths of motional blur in multiple observed images

From Eq.(6), it is obvious that only giving $(\Delta u^{(i)}, \Delta v^{(i)})$ is not sufficient to decide $(\Delta u^{(j)}, \Delta v^{(j)})$, this is to say, one observation PSF path is unable to determine another observation PSF path. It is necessary to know $(\Delta u^{(i)}, \Delta v^{(i)})$ and $d_1^{(i)}$. Here, we use the PSF paths of two observation i and j to estimate $d_1^{(i)}$ or $d_1^{(j)}$. Once obtaining $d_1^{(i)}$ or $d_1^{(j)}$, we can use $(\Delta u^{(i)}, \Delta v^{(i)}, d_1^{(i)})$ or $(\Delta u^{(j)}, \Delta v^{(j)}, d_1^{(j)})$ to compute any other observation PSF path.

If we have estimated the PSF paths of two observations, which can be estimated by blind deblurring algorithm, i.e. $\Delta \hat{u}^{(i)}$, $\Delta \hat{v}^{(i)}$ and $\Delta \hat{u}^{(j)}$, $\Delta \hat{v}^{(j)}$, substituting them into Eq. (6), we can get three equations with two unknown parameters $d_1^{(i)}$ and $d_1^{(j)}$, it is an overdetermined system of linear equation with two unknowns, then using the least square method, we can estimate $\hat{d}_1^{(i)}$, $\hat{d}_1^{(j)}$ with the least error easily.

When $\hat{d}_1^{(i)}$ and $\hat{d}_1^{(j)}$ are estimated, any other PSF path $(\Delta \hat{u}^{(n)}, \Delta \hat{v}^{(n)})$ can be calculated by following equations:

$$d_1^{(n)}=\begin{vmatrix} u_0^{(n)}+\Delta u^{(n)} \\ v_0^{(n)}+\Delta v^{(n)} \\ 1 \end{vmatrix} = [B^{(n)}]^{-1}\begin{vmatrix} \hat{b}_0 \\ \hat{b}_1 \\ \hat{b}_2 \end{vmatrix}, \ (n=0,1,\cdots,N-1) \quad (7)$$

where $\hat{b}_0$, $\hat{b}_1$, $\hat{b}_2$ are related with $\Delta \hat{u}^{(i)}$, $\Delta \hat{v}^{(i)}$, $\hat{d}_1^{(i)}$, and they can be computed by

$$\begin{vmatrix} \hat{b}_0 \\ \hat{b}_1 \\ \hat{b}_2 \end{vmatrix} = \hat{d}_1^{(i)}[B^{(i)}]\begin{vmatrix} u_0^{(i)}+\Delta \hat{u}^{(i)} \\ v_0^{(i)}+\Delta \hat{v}^{(i)} \\ 1 \end{vmatrix} - \begin{vmatrix} b_0 \\ b_1 \\ b_2 \end{vmatrix} \qquad (8)$$

In Eq. (7), there are three equations and three variables, so $\Delta \hat{u}^{(n)}$, $\Delta \hat{v}^{(n)}$, and $\hat{d}_1^{(n)}$ can be gotten by solving Eq. (7), and then PSF can be calculated by $psf_n=h(\Delta u^{(n)}, \Delta v^{(n)})$.

When object moves along a spatial curve path, its blur kernels in each observation are different curves. We discrete the PSF path by $u_k^{(i)}=u_0^{(i)}+\Delta u_k^{(i)}$, $v_k^{(i)}=v_0^{(i)}+\Delta v_k^{(i)}$, where k denotes the order of discrete points along the motional trajectory. After discretization of PSF paths, similar to straight line PSF

path, we can set up the relation of two observation PSF paths for these discrete corresponding points and estimate the depths of two observation $d_k^{(i)}$ and $d_k^{(j)}$ using the least square. And then we can estimate and refine the PSF paths of other observation.

4 Refinement optimization of PSFs and multiple observed images debluring

The values of two $\Delta \hat{u}^{(i)}$, $\Delta \hat{v}^{(i)}$ (supposing $i=1,2$) estimated by the proposed algorithm is not accurate, with only being precision of pixel level. The depths $\hat{d}^{(i)}$ to be calculated by the least square method in Eq.(6) is also rough. The precision of $\Delta \hat{u}^{(i)}$, $\Delta \hat{v}^{(i)}$ and $\hat{d}^{(i)}$ affect the accuracy of PSF paths of all observations, and then affect the quality of multiple observation deblurring. We define following minimizing square error criterion function to refine PSF paths to improve the accuracy,

$$E_m= \sum_i (|\Delta x_k^{(i+1)}-\Delta x_k^{(i)}|^2+|\Delta y_k^{(i+1)}-\Delta y_k^{(i)}|^2+|\Delta z_k^{(i+1)}-\Delta z_k^{(i)}|^2) \quad (9)$$

Taking two observations for example, the steps to refine PSF path are listed following:

(1) Obtaining $\Delta \hat{u}^{(i)}$, $\Delta \hat{v}^{(i)}$ (supposing $i=1,2$);

(2) Estimating $\hat{d}_k^{(i)}$ using Eq.(7) by the least square methods;

(3) Calculating $\Delta x_k^{(i)}, \Delta y_k^{(i)}, \Delta z_k^{(i)}$ and $\Delta x_k^{(i+1)}, \Delta y_k^{(i+1)}, \Delta z_k^{(i+1)}$, Substituting them into Eq.(9) to calculate the square error E_m;

(4) If the error is smaller than previous iterations, it can be accepted, otherwise jumped;

(5) Giving $\Delta \hat{u}_k^{(i)}$ and $\Delta \hat{v}_k^{(i)}$ some disturbances, $\Delta \hat{u}_k^{(i)} \leftarrow \Delta \hat{u}_k^{(i)}+\delta_u$, $\Delta \hat{v}_k^{(i)} \leftarrow \Delta \hat{v}_k^{(i)}+\delta_v$, where δ_u and δ_v are random Gaussion distribution variations with zero mean. Return to step (2).

When having estimated two PSF paths, the other PSF paths can be calculated and optimized by using the relationship of PSF paths in multiple observed images. Then, the deblur of the observed images can be removed using our proposed method. Once getting all deblurring images, the object can be easily

reconstructed well by the existing 3D reconstruction methods. The whole flow of three-dimension deblurring method is summarized in Fig.5.
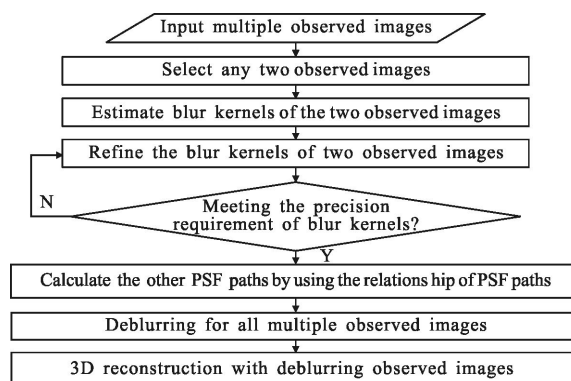

Fig.5 Flow chart of three-dimension deblurring method for multiple observed images

For multiple observed images with size $m \times m$, and total observation number is N, we give the analysis and comparison of computational complexities of independent deblurring method and proposed method respectively. The computational complexity of kernel estimation and latent image estimation of independent deblurring method is about $NA_k \times NA_i$, where A_k, A_i denote the computational complexity of kernel estimation and latent image estimation respectively. The computational complexity of proposed method main comes from the following three parts. (1) Kernel estimation of only two observed images, the computational complexity of this part is about $2A_k$; (2) PSF paths estimation of other observed images by Eq.(2)−(7), the computational complexity of this part is A_j, it depends on the dimensions of matrix which is much smaller than the image size $(m \times 3)$. Thus, the computational complexity of this part can be ignored; (3) Latent image estimation of all observed images, the computational complexity of this part is about NA_i. In conclusion, the computational complexity of proposed method and independent deblurring method is $2A_k+NA_i$ and NA_k+NA_i respectively, the ratio between them is $(2A_k+NA_i)/(NA_k+NA_i)$. Theoretically, when $N \times 2$, the computational time of proposed method is much less than independent deblurring method. In fact, the number is
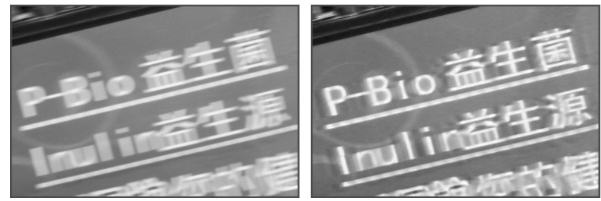
at least eight and more than twenty multiple observed images are required frequently.

5 Experiments results

The proposed three-dimension deblurring algorithm for stereo images have been programmed with VC6.0 language and implemented on the computer (Dell OptiPlex, 4G memory). We first test the effectiveness of estimating blur kernel from a single blurred image, because the first step of our method is to estimate two or three blur kernels using our method in Ref.[5]. It is critical to the following relationship determining. Fig.6(a) is an running bus scene image captured by a cannon camera Digital EOS 700D, Fig.6(b) is the deblurrred images and estimated blur kernel. The words on the bus wall are so blurred that we can not recognize them. To estimate the blur kernel quickly, we cut a part from the scene image, shown in Fig.6 (c). Using the single observed image deblurring method in Ref. [5], we have recovered image shown in Fig.6 (d). Obviously, the words have been recovered successfully and they can be recognized. The effectiveness of outdoor image debluring results shows that our work can efficiently remove motional blur and estimate the PSF path by using only one single image.

(c) Close-up observation of blurred image　(d) Close-up observation of deblurred image

Fig.6 Single observed image deblurring and PSF path estimation using our method

Next, we demonstrate the performance of our proposed method for multiple observed images. we use stereo images of an airplane with 24 observations. Multiple observation original images, blur images, recovered images by independent deblurring method and proposed method are listed in Fig.7(a)−7(c) respectively. Compared with the estimated blur kernel (in the box) in Fig.7 (b), the refined PSF paths in Fig.7(c) shows more sharply and accurately. This confirms that the proposed method can obtain accurate PSF paths. The deblurring results show that the characters and details in the deblurred images by proposed method are recovered well and distinct. The 3D reconstruction results of original images, blur images, recovered images by independent deblurring method and proposed method are shown in Fig.8(a)− 8(d) respectively, and corresponding close-up views of 3D surfaces are shown in red boxes in Fig.8(e)−8(h). Obviously, the characters and details are not apparent in the 3D surfaces of the 3D reconstruction in Fig.8(f). Compared with Fig.8(g), the characters in 3D surface in Fig.8 (h) are more readable, the details are richer and clearer. From these 3D reconstruction results, we

(a) Captured running bus image　(b) Deblurrred image and PSF path (in red box)
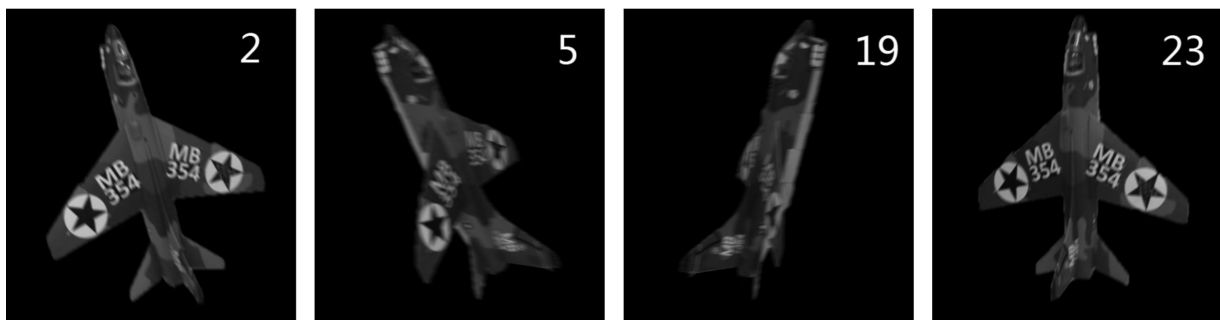
(a) Multiple observation blurred images of an airplane (total 24 observations)
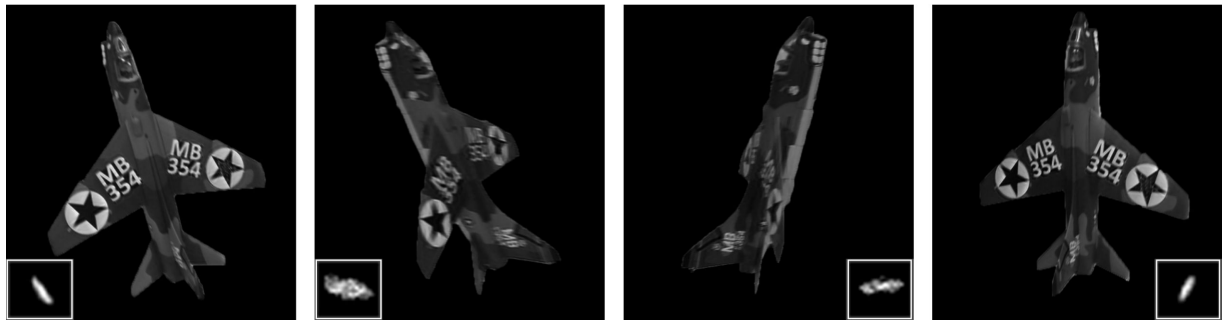
(b) Independent deblurring results for each observation image and estimated blur kernels (in boxes)
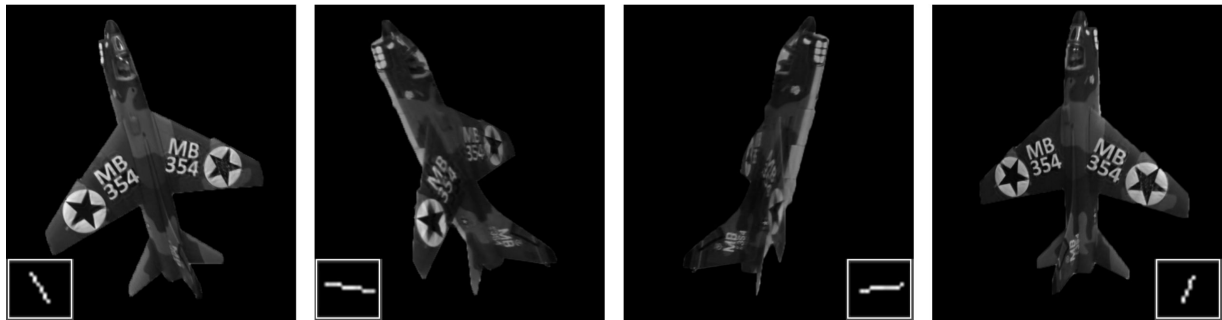
(c) Deblurred images with estimated PSF paths(in right bottom boxes) by proposed method

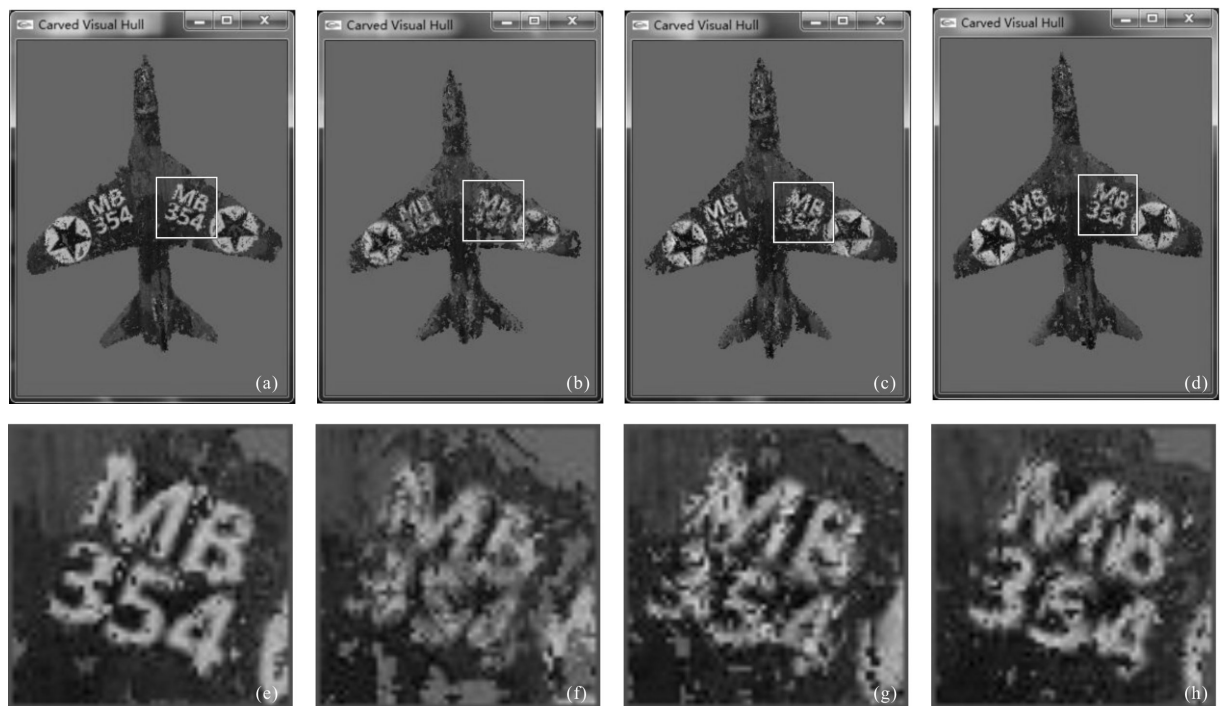Fig.7 Deblurring and PSF paths estimation for multiple observation images of an airplane

Fig.8 3D reconstruction for multiple observed images of an airplane. (a) 3D reconstruction using original images. (b) 3D reconstruction using blurred images. (c) 3D reconstruction using images deblurred by independent deblurring method[5]. (d) 3D reconstruction using deblurred images by proposed method. (e)−(h) Close−ups of 3D surfaces extracted from (a),(b),(c),(d) respectively (magnified for display by a factor of 3.6).

can see that information in the deblurring multiple observation images is recovered well, which indicates that our method provides significant improvements in the 3D reconstruction quality.

6 Conclusions

We have presented a three-dimension deblurring method for multiple observed images. The relationship of PSF paths of multiple observations has been set up. Once having estimated two observation PSF paths, the other observation PSFs can be calculated and optimized by using the relationship, then, our proposed algorithm can remove the blur of the all observations. Some 3D reconstruction experiment results show that our method provides significant improvements in the quality of 3D reconstruction. Future research directions for this work include two aspects: one is to make the estimation of multiple observation PSF paths to be more accu rate with higher precision, the other is how to recover more details from blurred images with less or no artifacts, with obtaining a higher precise 3D reconstruction.

References:

[1]   Joshi N, Szeliski R, Kriegman D J. PSF estimation using sharp edge prediction[C]//CVPR, 2008: 1−8.

[2]   Fergus R, Singh B, Hertzman n A, et al. Removing camera shake from a single photograph [J]. *ACM Transaction on Graphics (SIGGRAPH)*, 2006, 25(3): 787−794.

[3]   Jia J. Single image motion deblurring using transparency[C]// IEEE Conference on Computer Vision and Pattern Recognition(CVPR), 2007: 1−8, 17−22.

[4]   Shan Q, Xiong W, Jia J. Rotational motion deblurring of a rigid object from a single image [C]//ICCV, 2007: 10.1109/ICCV.2007.4408922.

[5]   Hong H, Park I K. Single-image motion deblurring using adaptive anisotropic regularization [J]. *Optical Engineering*, 2010, 49(9): 097008−1−097008−13.

[6]   Cho S, Matsushita Y, Lee S. Removing non-uniform motion blur from images[C]//ICCV, 2007: 10.1109/ICCV.2007.4408904.

[7]   Yuan L, Sun J, Quan L, et al. Image deblurring with blurred/noisy image pairs [J]. *ACM Trans on Graphics (SIGGRAPH)*, 2007, 26(3): 1−2.

[8]   Chen J, Yuan L, Tang C K, et al. Robust Dual Motion Deblurring[C]//CVPR, 2008.

[9]   Ben-Ezra M, Nayar S. Motion deblurring using hybrid imaging[C]//CVPR 2003, 1: 657−664.

[10]   Li F, Yu J, Chai J. A hybrid camera for motion deblurring and depth map super-resolution[C]//CVPR, 2008: 23−28.